

# Integrating Plug-and-Play Data Priors with Weighted Prediction Error for Speech Dereverberation

Ziye Yang, *Student Member, IEEE*, Wenxing Yang, Kai Xie, Jie Chen, *Senior Member, IEEE*

**Abstract**—Speech dereverberation aims to alleviate the detrimental effects of late-reverberant components. While the weighted prediction error (WPE) method has shown superior performance in dereverberation, there is still room for further improvement in terms of performance and robustness in complex and noisy environments. Recent research has highlighted the effectiveness of integrating physics-based and data-driven methods, enhancing the performance of various signal processing tasks while maintaining interpretability. Motivated by these advancements, this paper presents a novel dereverberation framework, which incorporates data-driven methods for capturing speech priors within the WPE framework. The plug-and-play strategy (PnP), specifically the regularization by denoising (RED) strategy, is utilized to incorporate speech prior information learnt from data during the optimization problem solving iterations. Experimental results validate the effectiveness of the proposed approach.

**Index Terms**—Speech dereverberation, the weighted prediction error method, data-driven method, learnt speech priors.

## I. INTRODUCTION

Speech signals captured in enclosed rooms by far-field microphones are inevitably affected by energy consumption and reflections from the room’s walls, ceilings, and other rigid objects during propagation. These effects result in delayed and attenuated copies of the source signal, known as speech reverberation. Reverberation causes degradation in the quality of the speech of interest, impacting various higher-level speech applications, including automatic speech recognition systems, speaker identification systems and teleconference systems [1]. Despite the challenge of differentiating the direct speech from its reverberation components, speech dereverberation has garnered significant attention.

Reverberation components can be categorized into early and late components based on the arrival time at the microphone array, which is influenced by factors such as room size, distance from the source to the microphones, and damping properties of the environment’s surfaces [2]. Typically, the subsequent 50 ms of the impulse response is considered as the early-reverberant components [3], while the remaining duration is referred to as the late-reverberant components. Research has shown that early-reverberant components are not perceptible to human hearing and improve the quality of the direct-path component [4]. Therefore, dereverberation techniques aim to eliminate the late-reverberant components while preserving the early-reverberant ones and the direct-path signal, as only the late-reverberant components have a detrimental effect on speech intelligibility and quality [5], [6].

A preliminary version has been accepted for European Signal Processing Conference (EUSIPCO 2023). This version provides detailed algorithm description and comprehensive experiments to illustrate the method.

The authors are with Center of Intelligent Acoustics and Immersive Communications, Northwestern Polytechnical University, China.

Considerable efforts have been devoted to devising speech dereverberation methods, which can be primarily categorized into conventional signal processing-based methods (i.e., physics-based methods) and data-driven algorithms. The former addresses the dereverberation problem based on the speech convolution model, with typical methods including acoustic channel equalization-based approaches [7], suppression-based methods [8], beamforming-based methods [9], and linear prediction-based methods [10]. These methods often model the acoustic transfer function as an autoregressive or convolutive problem [11]–[13], with the spectral coefficients of clean speech being modeled as a Gaussian or Laplacian distribution. Dereverberation is then performed by maximum likelihood estimation of unknown parameters [7]. When multiple microphones are available, spatial information can be leveraged to filter out signals arriving from undesired directions using beamforming algorithms [14]. For example, the work in [15] decomposes the multi-channel Wiener Filter into a minimum variance distortionless response and a single-channel post filter, enabling noise reduction and dereverberation in a two-stage approach. Among the numerous model-based dereverberation techniques, multichannel linear prediction (MCLP) methods, which estimate and subtract the late-reverberant components from the observed signal, show significant promise. One such method is the weighted prediction error (WPE) method [11], which has demonstrated its effectiveness in dereverberation. To further enhance performance, works such as [16] and [17] propose leveraging speech sparsity in the time-frequency domain to incorporate an additional prior on the unknown variance. Despite the clear physical interpretation of these model-based methods, their performance and robustness are limited as they do not fully exploit the inherent priors of speech signal structures.

In contrast, existing data-driven methods predominantly rely on deep learning and treat speech dereverberation as a supervised learning problem [18]. With large amounts of training data and increasing computational resources, data-driven methods have achieved state-of-the-art performance and have become a significant focus in the speech processing community. Initially, deep neural networks (DNNs) were trained to predict real-valued masks or magnitudes of the direct signal in the magnitude domain, with phases being utilized solely in the speech reconstruction stage [19], [20]. To better leverage spectral information, an extension was proposed, wherein the magnitude-domain masking and mapping method was adapted to the complex domain. This approach predicted the real and imaginary components of the direct-path signal from the received reverberant signals [14]. Subsequently, novel neural network architectures such as self-attention and recurrent networks were employed for end-to-end modeling in

other front-end speech processing tasks [21], [22]. Building on these advances, a monaural algorithm utilizing temporal convolutional networks with self-attention was proposed for end-to-end dereverberation in the time domain [23]. Data-driven methods, whether applied in the time-frequency or time domain, aim to learn a mapping function from input reverberant signals to output clear speech, incorporating speech priors into the network parameters. The powerful non-linear modeling capability of DNNs enables these methods to extract high-level features, leading to promising performance. However, they often neglect the explicit exploitation of the linear convolutional structure of reverberation [24], and the black-box nature of DNNs limits the physical interpretability of the entire speech recovery process.

Due to the respective merits and drawbacks of physics-based methods and data-driven methods, their integration has garnered significant attention in the signal processing community [25]–[27]. This integration benefits from both tractable mathematical modeling and highly-parameterized generic mappings tuned with large data. One promising strategy involves the plug-and-play technique (PnP), which incorporates a deep denoising algorithm as a module into the optimization iterations to capture data priors. The PnP strategy has been successfully investigated in various tasks, including inverse problems in image processing, which shares similar inherent problem formulations with the dereverberation problem. In these tasks, incorporating a denoiser implicitly characterizes image priors, enabling physics-based methods to solve inverse problems more effectively [28]–[33].

Inspired by these advances, we propose a framework for speech dereverberation that benefits from both physics-based models and data priors. In this work, we aim to incorporate data priors into the WPE framework from the perspective of formulating the optimization problem. We maintain the interpretability of the problem-solving process while integrating speech prior information learned from data. Specifically, we formulate the prediction error minimization problem of WPE with an additional regularizer that is not explicitly handcrafted. Unlike vanilla WPE and its extensions [16], [17], [34], [35], which do not consider sophisticated speech priors, we propose integrating speech prior information by employing the plug-and-play strategy. Specifically, we employ the regularization by denoising (RED) strategy, which is a promising variant of PnP [36]. We incorporate a pre-trained speech denoiser into the optimization iterations, and the proposed framework is referred to as PnPWPE. This approach effectively splits the speech processing problem into two distinct components: a model-based solving part and a data-prior capture part. By incorporating such a denoiser for the latter part, our framework harnesses the power of data-driven learning through denoiser training, eliminating the reliance on task-dependent data. This inherent flexibility makes our approach extendable for other speech processing tasks.

**Notation.** Normal font letters  $x$  and  $X$  denote scalars, and boldface small letters  $\mathbf{x}$  denote column vectors. Boldface capital letters  $\mathbf{X}$  represent matrices, and the operator  $(\cdot)^\top$  and  $(\cdot)^H$  denote matrix transpose and conjugate transpose respectively.  $\text{col}\{\cdot\}$  concatenates its vector arguments.

## II. SIGNAL MODEL AND VANILLA WPE METHOD

In this section, we first present the signal model in the reverberant scenario, followed by a description of the vanilla WPE method.

### A. Signal model for reverberant scenarios

Consider the scenario where a distant microphone array with  $Q$  channels captures the convolved speech. In time domain, the signal model of the  $q$ -th channel, indicating the relationship between the received reverberant speech  $b_q[t]$  and the target source signal  $s[t]$ , can be represented by

$$b_q[t] = s[t] * h_q[t] \quad (1)$$

where  $t$  indexes discrete time,  $*$  denotes the linear convolution, and  $h_q[t]$  is the acoustic impulse responses (AIRs) between the source and microphone. Equivalently, we can write (1) in vector form

$$b_q[t] = \mathbf{h}_q^\top \mathbf{s}[t], \quad (2)$$

with  $\mathbf{h}_q = (h_{q,0}, \dots, h_{q,L-1})^\top$ , and  $L$  being the order of AIR and  $\mathbf{s}[t] = (s[t], \dots, s[t-L+1])^\top$  is the speech signal vector.

If the AIRs i.e.,  $\mathbf{h}_q$ , from the source to microphone are available, the dereverberation problem can be formulated as an inverse problem in form of:

$$\min_{\mathbf{s}[t]} \sum_{t=1}^T |b_q[t] - \mathbf{h}_q^\top \mathbf{s}[t]|^2 + \mathcal{J}_{\text{reg}}(\{\mathbf{s}[t]\}_{t=1}^T). \quad (3)$$

with  $\mathcal{J}_{\text{reg}}$  being a regularizer which characterizes priors of  $\mathbf{s}[t]$ . Problem formulation (3) shares similarities with problems encountered in the image processing community, such as image deconvolution [37], which has been successfully addressed using the Plug-and-Play (PnP) strategy. However, applying an inverse filtering strategy for dereverberation presents challenges due to the estimate of AIRs [4]. Therefore, most recent work instead resort to the WPE formulation for dereverberation.

### B. Vanilla WPE method

The WPE algorithm belongs to the MCLP class and is typically applied in the frequency domain. The signal model described in Eq. (1) can be approximated in the Short-Time Fourier Transform (STFT) domain [11]

$$B_q(n, k) = \sum_{l=0}^{L-1} H_q(l, k) S(n-l, k), \quad (4)$$

where  $n$  and  $k$  are the time-frame and frequency bin indices respectively.  $B_q(n, k)$ ,  $S(n, k)$  and  $H_q(n, k)$  represent the counterparts of  $b_q[t]$ ,  $s[t]$  and  $h_{q,l}$  in STFT domain respectively. According to the theory of MCLP, the signal model can be converted to the following auto-regressive problem:

$$B_{\text{ref}}(n, k) = \hat{S}(n, k) + \bar{\mathbf{w}}^H(k) \bar{\mathbf{b}}(n-D, k), \quad (5)$$

where  $B_{\text{ref}}(n, k)$  is the reference signal randomly chosen at any microphone.  $\hat{S}(n, k)$  corresponds to the desired signal that consists the direct-path signal and early-reverberation component determined by prediction delay  $D$ . The regressor

$\bar{\mathbf{b}}(n-D, k)$  in frequency bin  $k$ , of length  $L_Q = L \times Q$ , is constructed by concatenating the regressors of all  $Q$  channels

$$\bar{\mathbf{b}}(n-D, k) = \text{col}\{\mathbf{b}_1(n-D, k), \dots, \mathbf{b}_Q(n-D, k)\} \quad (6)$$

with  $\mathbf{b}_q(n-D, k) = (B_q(n-D, k), \dots, B_q(n-D-L+1, k))^T$ .  $\bar{\mathbf{w}}(k)$  is the prediction filter of length  $L_Q$  in frequency bin  $k$ , constructed by concatenating prediction weights of each channel

$$\bar{\mathbf{w}}(k) = \text{col}\{\mathbf{w}_1(k), \dots, \mathbf{w}_Q(k)\} \quad (7)$$

with  $\mathbf{w}_q(k) = (W_q(0, k), \dots, W_q(L-1, k))^T$ . With an given  $\bar{\mathbf{w}}(k)$ , the prediction residual is considered as the desired signal that can be evaluated by:

$$\hat{S}(n, k) = B_{\text{ref}}(n, k) - \bar{\mathbf{w}}^H(k) \bar{\mathbf{b}}(n-D, k). \quad (8)$$

The WPE method aims to effectively determine the filter weight vector  $\bar{\mathbf{w}}(k)$ . Assuming that the desired signal follows a zero-mean complex Gaussian distribution with a time-varying variance  $\sigma(n, k)$ , the probability density function can be expressed as:

$$\begin{aligned} \mathcal{P}(\hat{S}(n, k)) &= \mathcal{N}_{\mathbb{C}}(\hat{S}(n, k); 0, \sigma(n, k)) \\ &= \frac{1}{\pi \sigma(n, k)} e^{-\frac{|\hat{S}(n, k)|^2}{\sigma(n, k)}} \end{aligned} \quad (9)$$

where  $\sigma(n, k)$  represents the Power Spectral Density (PSD) of the desired signal and is considered as an unknown parameter. Based on this physical model described in Equation (9), we can formulate the log-likelihood function for each independent frequency as:

$$\begin{aligned} \mathcal{L}(\bar{\mathbf{w}}(k), \boldsymbol{\sigma}(k)) &= \prod_{n=1}^N \mathcal{N}_{\mathbb{C}}(\hat{S}(n, k); 0, \sigma(n, k)), \\ &\text{for all } k = 1, \dots, K \end{aligned} \quad (10)$$

with  $\boldsymbol{\sigma}(k) = [\sigma(1, k), \sigma(2, k), \dots, \sigma(N, k)]^T$ . In order to estimate  $\bar{\mathbf{w}}(k)$  and  $\boldsymbol{\sigma}(k)$ , a maximum likelihood criterion is employed, leading to minimize the following cost function:

$$\begin{aligned} \mathcal{J}(\{\bar{\mathbf{w}}(k)\}_{k=1}^K, \{\boldsymbol{\sigma}(k)\}_{k=1}^K) \\ = \sum_{k=1}^K \sum_{n=1}^N \frac{|\hat{S}(n, k)|^2}{\sigma(n, k)} + \log \pi \sigma(n, k). \end{aligned} \quad (11)$$

The estimation of  $\bar{\mathbf{w}}(k)$  and  $\boldsymbol{\sigma}(k)$  can be performed iteratively. Given  $\boldsymbol{\sigma}(k)$ ,  $\bar{\mathbf{w}}(k)$  is obtained using a closed-form solution:

$$\bar{\mathbf{w}}(k) = [Z_{\bar{\mathbf{b}}}(k)]^{-1} \mathbf{q}_{\bar{\mathbf{b}}}(k), \quad (12)$$

where

$$Z_{\bar{\mathbf{b}}}(k) = \sum_{n=1}^N \frac{\bar{\mathbf{b}}(n-D, k) [\bar{\mathbf{b}}(n-D, k)]^H}{\sigma(n, k)} \quad (13)$$

and

$$\mathbf{q}_{\bar{\mathbf{b}}}(k) = \sum_{n=1}^N \frac{\bar{\mathbf{b}}(n-D, k) B_{\text{ref}}^*(n, k)}{\sigma(n, k)}. \quad (14)$$

Once  $\bar{\mathbf{w}}(k)$  is obtained, we can calculate  $\hat{S}(n, k)$  using Eq. (8) and subsequently estimate the PSD of  $\hat{S}(n, k)$  as:

$$\sigma(n, k) = \max\{|\hat{S}(n, k)|^2, \epsilon\} \quad (15)$$

with  $\epsilon$ , a lower bound needs to be predefined.

### III. PLUG-AND-PLAY FRAMEWORK FOR SPEECH DEREVERBERATION

In this section, we first reformulate the prediction error minimization problem of WPE to incorporate deep speech priors, and then present the solving method.

#### A. Problem formulation

In this work, we consider a multiple-input-single-output (MISO) scenario, that is, to calculate the filter weight through all received reverberant signals and to estimate the desired signal at a reference microphone that is randomly chose. Meanwhile, the received signal contains both reverberation and noise. Therefore, we assume the scenario where a  $Q$ -channel array captures the convolved speech with explicit ambient noise and thus the signal model should be defined by

$$\begin{aligned} x_q[t] &= b_q[t] + y_q[t] \\ &= h_q[t] * s[t] + y_q[t], \end{aligned} \quad (16)$$

where  $y_q[t]$  represents the additive noise independent of  $b_q[t]$ . Likewise, in STFT domain, (16) can be represented as

$$\begin{aligned} X_q(n, k) &= B_q(n, k) + Y_q(n, k) \\ &= \sum_{l=0}^{L-1} H_q(l, k) S(n-l, k) + Y_q(n, k), \end{aligned} \quad (17)$$

with  $Y_q(n, k)$  being the STFT representation of  $y_q[t]$ . Considering the MCLP process, the desired speech should be estimated by

$$R(n, k) = X_{\text{ref}}(n, k) - \bar{\mathbf{w}}^H(k) \bar{\mathbf{x}}(n-D, k) - V(n, k), \quad (18)$$

where  $V(n, k)$  is an estimate of the noise, and  $\bar{\mathbf{x}}(n-D, k)$  is constructed by the way similar to  $\bar{\mathbf{b}}(n-D, k)$  in Sec. II-B. The rationale of introducing  $V(n, k)$  will be elaborated in the next subsection and confirmed in the experiment. For notation simplicity, we also denote the prediction error without removing noise by:

$$\hat{S}(n, k) = X_{\text{ref}}(n, k) - \bar{\mathbf{w}}^H(k) \bar{\mathbf{x}}(n-D, k). \quad (19)$$

From Eq. (15), we can see that the time-varying variance  $\sigma(n, k)$  is related to the estimated signal and can be evaluated and inserted over iterations. Therefore, we denote the cost function related to WPE by:

$$\mathcal{J}_{\text{WPE}}(\{\bar{\mathbf{w}}(k)\}_{k=1}^K) = \sum_{k=1}^K \sum_{n=1}^N \frac{|\hat{S}(n, k)|^2}{\sigma(n, k)}, \quad (20)$$

Since the prediction error  $R(n, k)$  is considered as the desired signal, it is beneficial to introduce a regularization term to incorporate speech priors (with respect to  $R(n, k)$ ) for (20):

$$\mathcal{J}_{\text{WPE\_Reg}}(\{\bar{\mathbf{w}}(k)\}_{k=1}^K) = \mathcal{J}_{\text{WPE}}(\{\bar{\mathbf{w}}(k)\}_{k=1}^K) + \beta \mathcal{J}_{\text{Reg}}(\mathbf{R}), \quad (21)$$

where  $\beta$  is a trade-off parameter,  $\mathcal{J}_{\text{Reg}}$  denotes a regularizer, and  $\mathbf{R}$  is the speech time-frequency matrix consisting of  $\{R(n, k)\}_{n=1, k=1}^{N, K}$ .

<sup>1</sup>Note that the similar definition will be used for the other bold capital letters, such as  $\hat{\mathbf{S}}$ ,  $\mathbf{V}$  and  $\mathbf{P}$ .

Handcrafting a performant regularizer  $\mathcal{J}_{\text{Reg}}$  and finding an efficient solving method is not a trivial task. Instead, we propose to learn priors from speech data and incorporate them into the mathematics-based optimization based on the PnP strategy. The prototype PnP scheme, however, presents some complexities. The regularization is implicit as it involves a denoising algorithm, and careful parameter tuning is required during the PnP procedure, as the choice of the denoiser plugged into the framework affects the input noise-level of the denoising algorithm [36]. To ensure a more general regularization for our framework, we consider  $\mathcal{J}_{\text{Reg}}$  in the following form:

$$\mathcal{J}_{\text{Reg}}(\mathbf{R}) = \frac{1}{2} \langle \mathbf{R}, \mathbf{R} - \Omega(\mathbf{R}) \rangle, \quad (22)$$

where  $\Omega(\cdot)$  denotes an off-the-shelf denoiser. This specific form is known as RED [36], which has proven to be an effective regularizer. RED exhibits favorable derivative properties under mild assumptions, enabling it to effectively manage the gradient of the regularization term. Notably, the penalty itself is proportional to the inner product between the desired speech,  $\mathbf{R}$ , and its denoised residual,  $\mathbf{R} - \Omega(\mathbf{R})$ . This interpretation aligns with a speech-adaptive Laplacian. Incorporating this form (22), the cost function can be expressed as follows:

$$\begin{aligned} \mathcal{J}_{\text{WPE\_Reg}}(\{\bar{\mathbf{w}}(k)\}_{k=1}^K) \\ = \mathcal{J}_{\text{WPE}}(\{\bar{\mathbf{w}}(k)\}_{k=1}^K) + \frac{\beta}{2} \mathbf{R}^H [\mathbf{R} - \Omega(\mathbf{R})]. \end{aligned} \quad (23)$$

With the inclusion of this explicit regularization expression, our overall objective function becomes clear, well-defined, and more precise. This formulation offers flexibility in accommodating arbitrary denoising engines represented by  $\Omega(\cdot)$ .

### B. Solving with the variable splitting technique

To solve the problem in (23), we employ the augmented Lagrange technique on  $R(n, k)$ . This allows us to formulate the problem with additional equality constraints, resulting in the following full problem formulation:

$$\min_{\bar{\mathbf{w}}(k), \mathbf{R}, \mathbf{V}} \sum_{k=1}^K \sum_{n=1}^N \frac{|\hat{S}(n, k)|^2}{\sigma(n, k)} + \frac{\beta}{2} \mathbf{R}^H [\mathbf{R} - \Omega(\mathbf{R})]$$

$$\text{s.t. } R(n, k) = X_{\text{ref}}(n, k) - \bar{\mathbf{w}}^H(k) \bar{\mathbf{x}}(n - D, k) - V(n, k) \\ \text{for } n = 1, \dots, N \text{ and } k = 1, \dots, K, \quad (24)$$

We have two perspectives to further explain the rationale behind introducing the term  $V(n, k)$ .

- From a mathematical standpoint, the introduction of new variables  $V(n, k)$  helps to prevent the overdetermination issue in (24). To be specific, if we were to rewrite the constraints without the auxiliary term for each frequency, we have  $N \times K$  equality constraints, while the number of unknowns is  $L_Q \times K$ . The vanilla WPE problem is inherently overdetermined, which limits the effectiveness of adding extra regularization. This is unlike regular PnP based on (3), which is usually underdetermined in many applications. Therefore, we add  $\mathbf{V}$  with  $N \times K$  variables

so that the regularization has sufficient degree of freedom in the solution space.

- Furthermore, from a physical modeling perspective, we interpret  $\mathbf{R}$  as the clean output speech without any reverberation or noise. The vanilla WPE is specifically designed for speech dereverberation and is theoretically not suitable for speech denoising. To address this, we explicitly introduce the additive noise term during problem modeling and processing. By doing so, we aim to account for the presence of noise and maintain the physical interpretation in the formulation.

In order to facilitate the solving process, we convert the constrained problem to the unconstrained problem in (24) by the corresponding (scaled) augmented Lagrangian function, which is defined as:

$$\begin{aligned} \mathcal{L}(\bar{\mathbf{w}}(k)_{k=1}^K, \mathbf{R}, \mathbf{V}, \mathbf{P}) \\ = \mathcal{J}_{\text{WPE}} + \frac{\beta}{2} \mathbf{R}^H [\mathbf{R} - \Omega(\mathbf{R})] + \frac{\rho}{2} \sum_{k=1}^K \sum_{n=1}^N \left( |X_{\text{ref}}(n, k) - \bar{\mathbf{w}}^H(k) \right. \\ \left. \times \bar{\mathbf{x}}(n - D, k) - V(n, k) - R(n, k) + P(n, k) \right|^2 - |P(n, k)|^2 \Big), \end{aligned} \quad (25)$$

where  $P(n, k)$  is the scaled dual variable, and  $\rho$  is the penalty parameter. We then iteratively optimize the primal and dual variables of (25) by solving subproblems over iteration index  $\ell$  as follows.

- 1) Step 1 — Optimization with respect to  $\bar{\mathbf{w}}(k)$ : The optimization of (25) reduces to

$$\begin{aligned} \bar{\mathbf{w}}(k) = \underset{\bar{\mathbf{w}}(k)}{\text{argmin}} \mathcal{J}_{\text{WPE}} + \frac{\rho}{2} \sum_{k=1}^K \sum_{n=1}^N |X_{\text{ref}}(n, k) \\ - [\bar{\mathbf{w}}(k)]^H \bar{\mathbf{x}}(n - D, k) - V^{(\ell)}(n, k) \\ - R^{(\ell)}(n, k) + P^{(\ell)}(n, k)|^2. \end{aligned} \quad (26)$$

The optimization w.r.t.  $\bar{\mathbf{w}}(k)$  is a separable least square problem and can be then solved by

$$\bar{\mathbf{w}}^{(\ell+1)}(k) = [R_{\bar{\mathbf{x}}}^{(\ell+1)}(k)]^{-1} \mathbf{p}_{\bar{\mathbf{x}}}^{(\ell+1)}(k), \quad (27)$$

where

$$R_{\bar{\mathbf{x}}}^{(\ell+1)}(k) = \sum_{n=1}^N \frac{\bar{\mathbf{x}}(n - D, k) [\bar{\mathbf{x}}(n - D, k)]^H}{\lambda^{(\ell+1)}(n, k)} \quad (28)$$

and

$$\mathbf{p}_{\bar{\mathbf{x}}}^{(\ell+1)}(k) = \sum_{n=1}^N \frac{\bar{\mathbf{x}}(n - D, k) \tilde{X}^{(\ell+1)}(n, k)^*}{\lambda^{(\ell+1)}(n, k)}. \quad (29)$$

In the above solution,  $\lambda^{(\ell+1)}(n, k)$  is given by

$$\lambda^{(\ell+1)}(n, k) = \frac{2\sigma^{(\ell)}(n, k)}{2 + \rho\sigma^{(\ell)}(n, k)}, \quad (30)$$

where  $\sigma^{(\ell)}(n, k)$  is calculated by (15), and  $\tilde{X}^{(\ell+1)}(n, k)$  is given by

$$\begin{aligned} \tilde{X}^{(\ell+1)}(n, k) = X_{\text{ref}}(n, k) - \frac{\rho}{2} \lambda^{(\ell+1)}(n, k) [R^{(\ell)}(n, k) \\ + V^{(\ell)}(n, k) - P^{(\ell)}(n, k)]. \end{aligned} \quad (31)$$

By substituting  $\bar{\mathbf{w}}(k)$  of each band into (19), we can construct matrix  $\hat{\mathbf{S}}$  which will be used in the following steps.

- 2) Step 2 — Optimization with respect to  $\mathbf{R}$ : The optimization problem (25) now reduces to

$$\begin{aligned} \mathbf{R}^{(\ell+1)} = \underset{\mathbf{R}}{\operatorname{argmin}} \frac{\rho}{2} \|\hat{\mathbf{S}}^{(\ell+1)} - \mathbf{V}^{(\ell)} - \mathbf{R}^{(\ell)} + \mathbf{P}^{(\ell)}\|^2 \\ + \frac{\beta}{2} [\mathbf{R}^{(\ell)}]^\text{H} [\mathbf{R}^{(\ell)} - \Omega(\mathbf{R}^{(\ell)})]. \end{aligned} \quad (32)$$

From the perspective of RED [36], the prior properties of speech can be incorporated in (32) by applying a denoising processing to speech  $\tilde{\mathbf{R}}$  defined by

$$\tilde{\mathbf{R}}^{(\ell+1)} = \hat{\mathbf{S}}^{(\ell+1)} - \mathbf{V}^{(\ell)} + \mathbf{P}^{(\ell)}. \quad (33)$$

Setting the derivative of the above optimization w.r.t.  $\mathbf{R}$  to zero, we can minimize it directly by some iterative scheme, leading to the following equation:

$$\rho(\mathbf{R}^{(\ell)} - \tilde{\mathbf{R}}^{(\ell+1)}) + \beta(\mathbf{R}^{(\ell)} - \Omega(\tilde{\mathbf{R}}^{(\ell)})) = 0. \quad (34)$$

The solution to this problem can be achieved via the fixed-point iteration:

$$\rho(\mathbf{R}^{(\ell,i+1)} - \tilde{\mathbf{R}}^{(\ell+1)}) + \beta(\mathbf{R}^{(\ell,i+1)} - \Omega(\tilde{\mathbf{R}}^{(\ell,i)})) = 0 \quad (35)$$

leading to

$$\mathbf{R}^{(\ell+1,i+1)} = \mu \tilde{\mathbf{R}}^{(\ell+1)} + (1 - \mu)\Omega(\tilde{\mathbf{R}}^{(\ell,i)}; \Theta) \quad (36)$$

with  $\mu = \frac{\rho}{\rho + \beta}$  and inner iteration  $i = 1, \dots, I$ , where  $\Theta$  denotes the parameters of the denoiser.

- 3) Step 3 — Optimization with respect to  $\mathbf{V}$ : Here, the solution of this optimization problem readily writes

$$\mathbf{V}^{(\ell+1)} = \hat{\mathbf{S}}^{(\ell+1)} - \mathbf{R}^{(\ell+1)} + \mathbf{P}^{(\ell)}. \quad (37)$$

- 4) Step 4 — Update of  $\mathbf{P}$ : This dual variable is updated in the standard manner:

$$\mathbf{P}^{(\ell+1)} = \mathbf{P}^{(\ell)} + \hat{\mathbf{S}}^{(\ell+1)} - \mathbf{V}^{(\ell+1)} - \mathbf{R}^{(\ell+1)}. \quad (38)$$

Variables  $\bar{\mathbf{w}}(k)$ ,  $\mathbf{R}$ ,  $\mathbf{V}$  and  $\mathbf{P}$  are updated until convergence, and output  $\mathbf{R}$  will be used as the estimated speech.

#### IV. EXPERIMENTS

In this section, we first present the DNN-based denoisers inserted in PnPWPE, then introduce the comparison methods and evaluation metrics utilized in our experiments, and finally validate the effectiveness of PnPWPE in several respects.

##### A. Data-driven prior construction

Benefiting from the generalization ability of the proposed framework, any denoiser can be plugged into it to incorporate speech priors. In order to illustrate such flexibility of our framework, in this work, we apply 4 different kinds of DNN-based denoisers trained by different datasets. The network structure diagrams are depicted in Fig. 1 and training details are summarized in Table I. In particular, we initially train a time-frequency (T-F) domain-based denoiser for illustrative purposes. Subsequently, we integrate three pre-trained and

---

**Algorithm 1:** Plug-and-play framework for speech dereverberation.

---

**Input:** The observed multi-channel

speech:  $\bar{\mathbf{x}}(n - D, k)$

**Output:** The estimated speech:  $\mathbf{R}$

**Parameters:** The time delay:  $D$ ; The filter order:  $L$ ;

The lower bound:  $\epsilon$ ; The inner iterations:  $I$ ; The

penalty parameter of ADMM:  $\rho$ ; The parameter of the fixed-point algorithm:  $\mu$

**Initialize:** The auxiliary variables:  $\mathbf{V} = \mathbf{0}_{N \times K}$ ; The

dual variables:  $\mathbf{P} = \mathbf{0}_{N \times K}$ ; The predicted filter

weight vector:  $\bar{\mathbf{w}}(k) = \mathbf{0}_{L_Q \times 1}$ .

**while** *not converged* **do**

**for**  $k = 1$  **to**  $K$  **do**

**for**  $n = 1$  **to**  $N$  **do**

      Calculate  $\sigma^{(\ell+1)}(n, k)$  by (15);

      Calculate  $\lambda^{(\ell+1)}(n, k)$  by (30);

      Calculate  $\tilde{X}^{(\ell+1)}(n, k)$  by (31);

**end**

    Calculate  $R_{\bar{\mathbf{x}}}^{(\ell+1)}(k)$  by (28);

    Calculate  $\mathbf{p}_{\bar{\mathbf{x}}}^{(\ell+1)}(k)$  by (29);

    Update  $\bar{\mathbf{w}}(k)^{(\ell+1)}$  by (27);

**end**

  Update  $\hat{\mathbf{S}}^{(\ell+1)}$  by (19);

  Update  $\tilde{\mathbf{R}}^{(\ell+1)}$  by (33);

**for**  $i = 1$  **to**  $I$  **do**

    Update  $\mathbf{R}^{(\ell+1,i)}$  by (36) (denoising);

**end**

  Update  $\mathbf{V}^{(\ell+1)}$  by (37);

  Update  $\mathbf{P}^{(\ell+1)}$  by (38);

$\ell = \ell + 1$

**end**

---

open-source complex domain denoisers into our framework. This approach showcases the versatility of our framework in accommodating various denoisers and leveraging their capabilities to enhance speech quality.

1) *BLSTM-based denoiser:* As illustrated in Fig. 1(a), we train a bidirectional long short-term memory (BLSTM)-based denoiser to predict the phase sensitive mask (PSM, [18]) for target speech via the magnitude and temporal spectrum approximation loss, defined by [43]

$$\begin{aligned} \mathcal{J}_{\text{Denoiser}} = \frac{1}{N} \sum \left( \|\hat{\mathbf{M}} \odot |\mathbf{Z}| - |\mathbf{A}| \odot \cos(\theta_{\mathbf{Z}} - \theta_{\mathbf{A}})\|_F^2 \right. \\ \left. + w_d \|f_d(\hat{\mathbf{M}} \odot |\mathbf{Z}|) - f_d(|\mathbf{A}| \odot \cos(\theta_{\mathbf{Z}} - \theta_{\mathbf{A}}))\|_F^2 \right. \\ \left. + w_c \|f_c(\hat{\mathbf{M}} \odot |\mathbf{Z}|) - f_c(|\mathbf{A}| \odot \cos(\theta_{\mathbf{Z}} - \theta_{\mathbf{A}}))\|_F^2 \right), \end{aligned} \quad (39)$$

where  $\hat{\mathbf{M}}$  denotes the predicted PSM,  $\odot$  is the Hadamard product,  $|\mathbf{Z}|$  and  $|\mathbf{A}|$  are the magnitude of noisy and clean speech, and  $\theta_{\mathbf{Z}}$  and  $\theta_{\mathbf{A}}$  represent phase angles of noisy speech and the clean speech respectively.

Taking the dynamic information into consideration, we employ the functions (i.e.,  $f_d(\cdot)$  and  $f_c(\cdot)$ ) to calculate increment and acceleration, the increment computation function

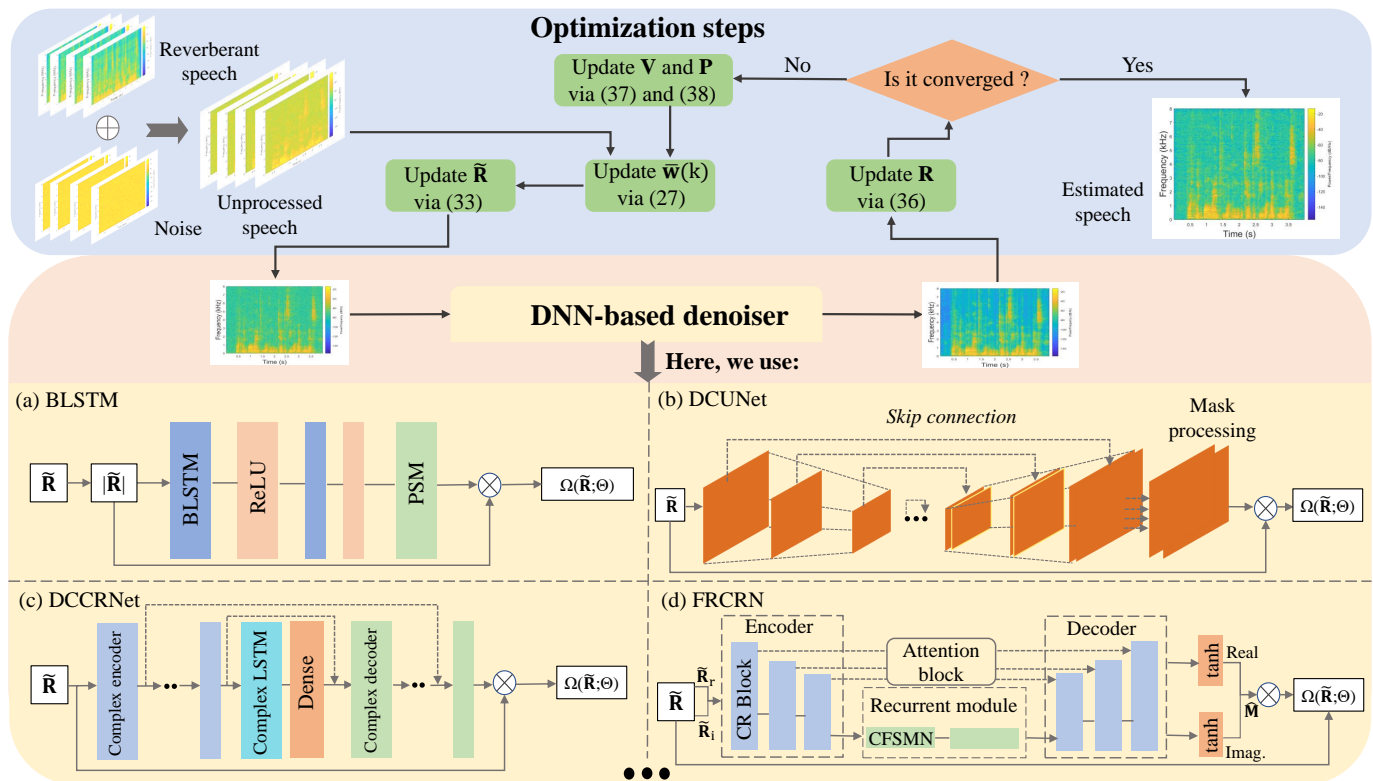


Fig. 1. Diagram of PnPWPE. The upper part illustrates the optimization steps of our proposed framework, and the bottom part shows the way we insert the DNN-based denoiser into PnPWPE as well as network structures of denoisers we utilized in this work.

TABLE I  
DETAILS ABOUT DNN-BASED DENOISERS WHICH ARE PLUGGED INTO THE PROPOSED FRAMEWORK.

DNN-based denoiser	Dereverberation	Denoise	Domain	Training dataset	Neural network
BLSTM	✗	✓	Time-frequency	WSJ0Mix	Bidirectional Long Short-term Memory Network
DCUNet [38]	✗	✓	Complex	Libri1Mix [39]	Deep Complex U-net (Large-DCUNet-20)
DCCRNet [40]	✗	✓	Complex	Libri1Mix	Deep Complex CRN
FRCRN [41]	✓	✓	Complex	DNS-Challenge [42]	Frequency Recurrent CRN

is defined by

$$f_d(c[n]) = \frac{\sum_{o=1}^O o \times (c[n+o] - c[n-o])}{\sum_{o=1}^O 2o^2}, \quad (40)$$

where  $c[n]$  denotes the magnitude of a time frame, and  $O$  represents the contextual window which is set to 2. The acceleration function can be calculated by computing the increment twice. The weights  $w_d$  and  $w_c$  are set to 4.5 and 10.0 respectively.

To train a blind BLSTM-denoiser, we add the diffuse noise set, containing white Gaussian noise (WGN), babble noise, cafe noise, factory noise and bus noise chosen from NOISE-92 database [44] and chime-3 dataset [45], to the clean speech signals which are randomly chosen from the Wall Street Journal dataset (WSJ0, [46]). Then, we obtain a dataset termed WSJ0Mix, where the training set contains 20,000 utterances and the validation set contains 5000 utterances at various signal-noise ratios (SNRs) between -5 dB and 40 dB. Each utterance in WSJ0Mix is split into 4 seconds with a sampling rate of 16 kHz. We implement the BLSTM-based denoiser based on Adam optimizer [47] with an initial learning rate of

0.0005 and a mini-batch of 32 to minimize the loss function (39) in 60 epochs.

2) *DCUNet-based denoiser*: Deep Complex U-Net (DCUNet) is trained to estimate complex ratio mask for target speech based on a variant of U-Net [48]. As illustrated in Fig. 1(b), DCUNet consists of a complex convolutional autoencoder with skip-connections. In our work, we insert larger DCUNet-20 (Large-DCUNet-20)<sup>2</sup> trained by libri1mix dataset into our framework since the authors in [38] claim that this network with more channels in each layer outperforms other architectures.

3) *DCCRNet-based denoiser*: Deep Complex Convolution Recurrent Network (DCCRNet) [40] conducts complex-valued speech enhancement via the convolutional encoder-decoder (CED) architecture with a complex LSTM layer between the encoder and the decoder, as shown in Fig. 1(c). DCCRNet not only benefits from 2D convolution layer (Conv2d) to extract high-level features for better enhancement but also benefits from LSTM to model temporal context with less

<sup>2</sup>The open-source DCUNet is available at [https://huggingface.co/JorisCos/DCUNet\\_Libri1Mix\\_enshsingle\\_16k](https://huggingface.co/JorisCos/DCUNet_Libri1Mix_enshsingle_16k).

parameters. Here, we plug DCCRN-CL<sup>3</sup> which is also trained by Libri1Mix dataset into our framework.

4) *FRCRN-based denoiser*: Frequency Recurrent Convolutional Recurrent Networks (FRCRN), as shown in Fig. 1(d), is trained to predict complex ideal ratio mask for target speech via an extended CED architecture, known as convolutional recurrent encoder-decoder structure which is able to improve feature representation. In addition, the recurrent module and attention block of FRCRN are designed to model the long-term temporal dependencies and to facilitate information flow respectively. The FRCRN model<sup>4</sup> we insert into our framework is trained by Deep Noise Suppression (DNS)-Challenge dataset [42], of which 30% of dataset contains reverberant components.

Once the denoiser has been already pre-trained, it can be directly plugged into the proposed framework, yielding Algorithm 1.

## B. Method comparison and evaluation

1) *Comparison method*: Our objective is to enhance the performance of the vanilla WPE algorithm in complex environments. Therefore, in our experiments, we consider the vanilla WPE as the baseline for comparison.

Since our experimental scenarios involve both additive noise and reverberation, we also explore a straightforward concatenation of denoising and dereverberation algorithms to ensure a fair comparison. We introduce two comparison methods, denoted by Denoise+WPE and WPE+denoise, with different orderings of the algorithms. In the Denoise+WPE approach, we initially apply the denoising algorithm to each channel of the unprocessed speech signals. The enhanced signals from all channels are then concatenated along the channel axis to obtain a multi-channel signal, which is further processed by the vanilla WPE algorithm. On the other hand, for WPE+denoiser, considering the MISO (Multiple-Input Single-Output) characteristic of the WPE method, we apply the single-channel dereverberated signal to the denoising algorithm after applying the vanilla WPE. To ensure a fair comparison, the denoising algorithms used in these approaches are the same ones we integrate into our proposed framework.

Apart from simple combination of denoising and dereverberant algorithms, we compare our proposed framework with convolutional time-domain audio separation network (Conv-TasNet) [49], an end-to-end time domain speech separation algorithm. We utilize an open-source Conv-TasNet model<sup>5</sup> to directly process the test set. Since this model has been pre-trained by the single-speaker version of WHAMR! [50] with corpus containing noise and reverberation, it is considered as a pure dataneural-network (NN) comparison method in our experiments.

<sup>3</sup>The open-source DCCRNNet is available at [https://huggingface.co/JorisCos/DCCRNNet\\_Libri1Mix\\_enhsingle\\_16k](https://huggingface.co/JorisCos/DCCRNNet_Libri1Mix_enhsingle_16k).

<sup>4</sup>The open-source FRCRN is available at [https://www.modelscope.cn/models/damo/speech\\_frmc\\_ans\\_cirm\\_16k](https://www.modelscope.cn/models/damo/speech_frmc_ans_cirm_16k).

<sup>5</sup>The open-source Conv-TasNet is available at [https://huggingface.co/cankeles/ConvTasNet\\_WHAMR\\_enhsingle\\_16k](https://huggingface.co/cankeles/ConvTasNet_WHAMR_enhsingle_16k).

TABLE II  
PARAMETER SETTING OF GENERATING TEST SETS.

Room type	Room A	Room B
Room length (m)	8-13	15-20
Room width (m)	8-13	15-20
Room height (m)	2.8-3.8	3-4
T60 (ms)	400-800	800-1200
Minimum distance from source to wall (m)	0.5	0.8
Minimum distance from source to microphone (m)	0.8	1.3
Microphone array	Linear array with 4 channels	
	Inner distance = 40 mm	
	Microphone type = Omnidirectional	

2) *Evaluation metrics*: For evaluation metrics, we adopt three widely used measures for speech dereverberation, i.e., perceptual evaluation of speech quality (PESQ) [51], cepstral distance (CD) [52] and frequency-weighted segmental signal-to-noise ratio (F-SNR) [52] in our experiments. In general, for PESQ and F-SNR, larger values indicate better performance, while for CD, smaller values indicate better performance. To explicitly show the convergence of proposed framework, we define energy error between the left and right sides of the constraint of (24):

$$\text{Error} = \frac{1}{NK} \sum_{n=1}^N \sum_{k=1}^K |R(n, k) - \hat{S}(n, k) - V(n, k)|^2. \quad (41)$$

## C. Results

1) *Dataset description*: To test the proposed framework, we generate a test set by simulating random reverberant scenarios. Specifically, we randomly generate 4 microphones in two types of rooms, denoted as Room A and Room B, corresponding to different room size ranges. The microphone array and speech source are located randomly within the rooms. More details can be found in Table II. We create room impulse responses (RIRs) using the method in [53]. We split 20 clean speech signals, randomly chosen from the Librispeech corpus [54], into 4-second segments with a sampling rate of 16 kHz. We then convolve them with the RIRs, where the reverberant time ( $T_{60}$ ) is constrained within the range of 400-800 milliseconds (ms) for Room A and 800-1200 ms for Room B.

In addition, we evaluate the robustness of the proposed framework under noisy and reverberant conditions. As widely demonstrated in image processing based on PnP, this strategy to excavate deep priors is able to yield promising results with White Gaussian Noise (WGN). However, for speech signal processing, it is insufficient to only test the performance in the case of WGN, and thus we consider more scenarios. In our experiments, we choose three additive noises, namely WGN, babble, and cafe, chosen from the diffuse noise set (mentioned in Sec. IV-A), and further add them to the reverberant speech signals. We set the Signal-to-Noise Ratios (SNRs) to 0 dB, 10 dB, and 20 dB, respectively. This way, we obtain a test set of 18 experimental scenarios and a total of 360 utterances. To avoid the randomness of the results, we evaluate the methods on the test set and take the average value.

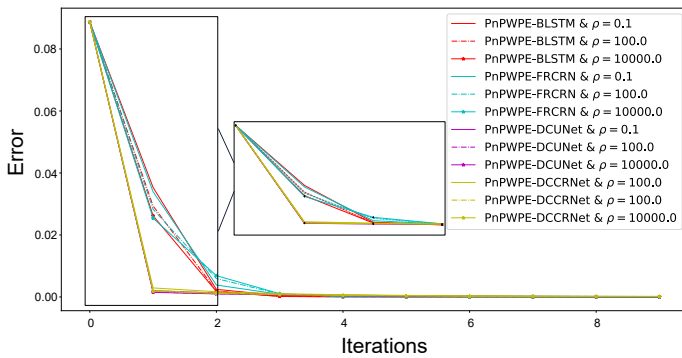


Fig. 2. The Error convergence curves of the proposed framework in terms of different settings of  $\rho$  in the scenario with WGN at SNR = 0 dB in Room B.

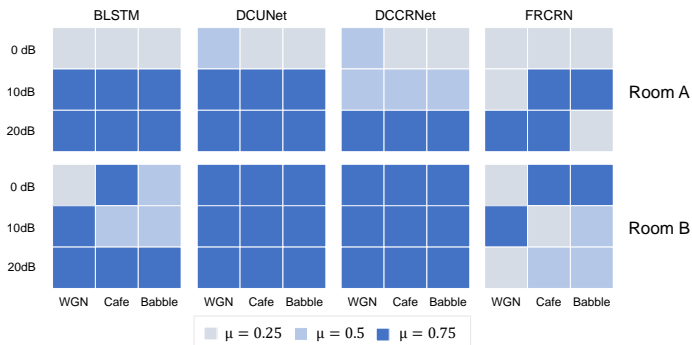


Fig. 3. The settings of  $\mu$  in different scenarios, where each  $3 \times 3$  square denotes PnPWPE inserted with a kind of DNN-based denoiser.

2) *Experimental settings*: The proposed framework is implemented in the STFT domain using a Hann window, where the frame length is 32 ms of 75% overlapping. For MCLP process, considering the trailing effect of reverberation, the filter order  $L$  is set to 28 for Room A and 35 for Room B. In addition, we set the time delay  $D$  to 2 and choose the first microphone as the reference microphone in all experiments. For calculating  $\sigma$  in (15), the lower bound  $\epsilon$  is set to 0.0001. For simplicity, we set the inner iteration  $I$  to 1 to speed the overall framework. The penalty parameter  $\rho$  in the augmented Lagrangian function only affects the convergence speed, as theoretically shown [32] and experimentally shown in Fig. 2. Therefore we simply set  $\rho = 0.1$  in our experiments. As for the trade-off parameter  $\mu$  in the fixed-point iteration controlling the impact of the denoising engine, we first choose a relatively suitable setting on a single signal for each experimental scenario, and then apply the selected setting to all test sets. The specific settings of  $\mu$  are summarize in Fig. 3.

3) *Results discussion*: Table III and Table IV summarize the comparison results of all evaluation metrics in Room A and Room B respectively. For visual comparison, we take the scenarios SNR = 10 dB and 20 dB of WGN in Room A and SNR = 20 dB of cafe in Room B as examples, depicted in Fig. 4. From overall results, we can briefly draw conclusions on the proposed method as follows:

- Our proposed framework is flexible with different denoisers. We observe that for each denoiser, PnPWPE outperforms other combination strategies in most cases. It is worth noting that the DNN-based denoisers we utilized were trained using datasets with various settings. This implies that PnPWPE provides an efficient approach to

seamlessly integrate any pre-trained denoiser into the WPE framework in practical applications. Furthermore, we made an interesting discovery that PnPWPE-FRCRN consistently delivers the best results. This can be attributed to the fact that, compared to the other three denoisers, FRCRN was trained using a larger and more complex dataset.

- Our proposed framework leverages prior information extracted by DNN-based denoisers, effectively enhancing the quality of reconstructed speech signals in environments characterized by both reverberation and noise. Notably, the performance of PnPWPE-type methods stands out prominently when considering scenarios involving white Gaussian noise (WGN). Table III clearly demonstrates that these methods consistently achieve the best and second-best results. In the case of additive noises in the other two scenarios, while PnPWPE-type methods display some variability in terms of F-SNR values, they still outperform the comparison methods across other evaluation metrics. Moreover, PnPWPE exhibits robustness across different SNRs and reverberation times. Even in challenging conditions characterized by low SNRs and high levels of reverberation, our proposed method maintains its superiority.

In what follows, we will first discuss the results between PnPWPE and different types of comparison methods in detail. Then, we will show the usefulness of introducing the term  $V(n, k)$ , and discuss the convergence property of PnPWPE.

**Comparison of PnPWPE and the vanilla WPE**: From Table III and Table IV, we can see that the proposed PnPWPE shows superiority compared to the vanilla WPE, especially in the scenario with WGN. Specifically, PnPWPE-FRCRN outperforms the vanilla WPE relatively by **20.7 % (1.313  $\rightarrow$  1.972)**, **21.8 % (1.870  $\rightarrow$  2.444)** and **17.6 % (2.281  $\rightarrow$  2.672)**<sup>6</sup> about PESQ at SNR = 0 dB, 10 dB, 20 dB in Room A, For Room B, the relative improvements of PESQ are **18.4 % (1.217  $\rightarrow$  1.821)**, **14.0 % (1.687  $\rightarrow$  2.080)** and **8.0 % (2.135  $\rightarrow$  2.325)** at SNR = 0 dB, 10 dB, 20 dB respectively. In addition, Fig. 4 shows that the vanilla WPE can not work well under the scenarios with WGN, especially at lower SNRs.

As for more lifelike scenarios, we can observe that, in the cases with cafe and babble which contain the sound of tableware colliding and the chattering of people, the proposed PnPWPE still maintains its advantages compared to the vanilla WPE, as all the evaluation metrics of the former is higher than those of the latter. Actually, it has been found that WPE-type methods are not robust to additive noise [55]. Our results support this view and further demonstrate the necessity of inserting speech prior for WPE to boost the robustness of the vanilla WPE under such complex environments.

**Comparison of PnPWPE and Conv-TasNet**: From the presented results in Table III and Table IV, it can be seen that PnPWPE performs better than Conv-TasNet in most cases. Despite the fact that the F-SNR value of Conv-TasNet is slightly higher than that of PnPWPE-type methods in the

<sup>6</sup>The relative improvement is calculated by:  $\Delta_{\text{relative}} = \frac{\text{PESQ}_1 - \text{PESQ}_2}{4.5 - \text{PESQ}_2}$  where 4.5 is the upper bound of PESQ.



TABLE III

THE RESULTS OF ALL COMPARISON METHODS IN ROOM A WITH ALL TYPES OF NOISES OF DIFFERENT LEVELS IN ROOM A. THE BEST RESULTS ARE IN BOLD AND THE SECOND BEST RESULTS ARE UNDERLINED.

Additive noise type	Noise level		SNR = 0 dB			SNR = 10 dB			SNR = 20 dB			
	Method	Denoiser	PESQ	CD	F-SNR	PESQ	CD	F-SNR	PESQ	CD	F-SNR	
WGN	Unprocessed	-	1.420	8.474	4.720	1.933	7.974	5.724	2.076	6.692	6.311	
	WPE	-	1.313	8.628	4.338	1.870	8.351	5.735	2.281	7.265	7.366	
	Conv-TasNet	-	1.353	9.043	4.784	1.917	8.255	5.837	2.015	7.182	5.938	
	Denoise + WPE	BLSTM		1.563	8.626	4.638	1.957	8.275	5.646	2.538	7.173	7.074
		DCUNet		1.284	8.522	4.666	1.653	8.074	5.740	2.025	6.765	6.559
		DCCRNNet		1.165	8.505	4.693	1.932	8.044	5.701	1.906	6.766	6.455
		FRCRN		<u>1.948</u>	8.550	4.558	2.221	8.237	5.689	2.453	6.998	6.480
	WPE + Denoise	BLSTM		1.486	7.938	3.998	1.832	7.358	5.156	2.240	6.441	5.985
		DCUNet		1.467	8.877	4.917	2.062	8.099	6.181	2.586	7.303	6.495
		DCCRNNet		1.104	8.678	4.225	1.861	9.357	5.731	2.296	8.327	6.079
		FRCRN		1.936	6.816	5.873	2.261	6.651	6.157	2.651	<u>6.154</u>	6.524
	PnPWPE	BLSTM		1.695	<u>6.789</u>	<u>6.353</u>	<u>2.287</u>	<u>6.812</u>	<b>7.397</b>	<u>2.659</u>	<b>5.328</b>	7.837
		DCUNet		1.407	8.444	5.122	2.175	7.705	6.746	2.642	6.239	7.678
		DCCRNNet		1.202	8.889	4.785	2.034	8.363	6.472	2.535	6.656	7.651
		FRCRN		<b>1.972</b>	<b>6.342</b>	<b>6.378</b>	<b>2.444</b>	<b>5.687</b>	<u>7.145</u>	<b>2.672</b>	<b>5.328</b>	<u>7.838</u>
	Cafe	Unprocessed	-	1.312	6.919	3.036	2.035	6.194	4.596	2.083	5.473	6.066
WPE		-	1.629	7.045	2.934	2.028	6.186	4.685	2.321	4.746	6.733	
Conv-TasNet		-	1.527	6.905	4.544	1.981	6.135	5.558	2.232	5.430	6.503	
Denoise + WPE		BLSTM		1.042	6.868	2.847	1.714	6.245	4.352	2.334	5.190	6.143
		DCUNet		1.354	6.938	2.983	2.019	6.209	4.465	2.139	5.267	6.100
		DCCRNNet		1.321	6.917	3.015	1.870	6.205	4.437	2.001	5.394	6.013
		FRCRN		1.699	7.027	3.095	2.064	6.318	4.548	2.334	5.516	6.101
WPE + Denoise		BLSTM		0.965	8.195	3.290	1.690	7.174	5.035	2.317	5.137	6.827
		DCUNet		1.669	7.822	4.113	2.129	7.310	5.481	2.481	6.238	7.227
		DCCRNNet		1.579	8.489	<b>4.887</b>	1.673	7.201	5.918	2.313	7.258	6.790
		FRCRN		1.704	<u>6.444</u>	<u>4.816</u>	2.197	5.914	5.999	<u>2.577</u>	4.722	<u>7.463</u>
PnPWPE		BLSTM		1.541	6.791	3.623	2.240	5.834	5.622	2.452	4.544	7.324
		DCUNet		1.578	6.711	4.046	<u>2.327</u>	5.629	5.775	2.545	<u>4.450</u>	7.213
		DCCRNNet		<u>1.824</u>	6.850	4.790	2.254	<u>5.524</u>	6.149	2.477	4.504	7.251
		FRCRN		<b>1.880</b>	<b>6.335</b>	4.406	<b>2.335</b>	<b>5.519</b>	5.733	<b>2.579</b>	<b>4.334</b>	7.342
Babble		Unprocessed	-	1.324	6.815	2.952	1.935	6.095	4.479	2.066	5.612	5.599
	WPE	-	1.317	7.011	2.620	2.014	5.818	4.311	2.421	4.676	6.216	
	Conv-TasNet	-	1.181	7.239	<b>4.173</b>	1.978	6.008	5.577	2.062	5.428	6.077	
	Denoise + WPE	BLSTM		1.221	6.907	2.984	1.654	6.097	4.139	2.110	5.416	5.503
		DCUNet		1.061	6.865	2.813	1.476	5.975	4.245	2.106	5.325	5.581
		DCCRNNet		1.138	6.856	2.801	1.977	6.012	4.227	2.080	5.459	5.556
		FRCRN		1.571	6.894	2.766	2.134	6.156	4.308	2.480	5.690	5.510
	WPE + Denoise	BLSTM		0.989	7.946	3.674	1.659	6.741	5.269	2.453	5.321	7.097
		DCUNet		1.092	8.172	3.567	2.085	7.020	5.497	2.596	6.043	7.188
		DCCRNNet		1.248	8.627	3.747	1.981	7.552	5.527	2.436	7.603	6.574
		FRCRN		1.307	6.868	3.847	<u>2.236</u>	<u>5.050</u>	<b>6.269</b>	<u>2.626</u>	<u>4.037</u>	<u>7.629</u>
	PnPWPE	BLSTM		1.523	<u>6.542</u>	<u>4.025</u>	2.114	5.283	5.610	<b>2.682</b>	4.257	7.156
		DCUNet		1.311	7.047	3.495	2.168	5.649	5.083	2.611	4.677	6.682
		DCCRNNet		<b>1.626</b>	7.076	3.941	2.205	5.681	5.477	2.589	4.504	7.251
		FRCRN		<u>1.621</u>	<b>6.528</b>	3.597	<b>2.274</b>	<b>4.883</b>	6.216	2.554	<b>4.025</b>	7.550

scenarios with babble in Room A at SNR = 0 dB, the PESQ and CD value of PnPWPE exceed Conv-TasNet (such as Conv-TasNet V.S. PnPWPE-BLSTM: **1.181**→**1.523**, **7.239**→**6.542**). The same trend can be found under the cafe noise in Room B at SNR = 0 dB. The main reason why PnPWPE performs more stably than Conv-TasNet may be that the data-driven module in our framework, i.e., the DNN-based denoiser, is to capture speech prior to boost the whole recovery process rather than directly reconstruct the desired speech from the received speech. Therefore, PnPWPE avoids excessive dependence on

specific data sets, which is a major factor that leads to poor generalization ability for pure data-driven methods.

From the explicit results in Fig. 4, we can find that Conv-TasNet is able to recover clean speech from reverberant and noisy conditions to some extent, but the estimated speech still retains some additive noise that cannot be removed. Taking the scenarios with WGN as an example, we can clearly see that the estimated speech generated by PnPWPE is more consistent with the ground truth compared to Conv-TasNet.

**Comparison of PnPWPE, Denoise+WPE and**

TABLE IV  
THE RESULTS OF ALL COMPARISON METHODS WITH ALL TYPES OF NOISES OF DIFFERENT LEVELS IN ROOM B. THE BEST RESULTS ARE IN BOLD AND THE SECOND BEST RESULTS ARE UNDERLINED.

Additive noise type	Noise level		SNR = 0 dB			SNR = 10 dB			SNR = 20 dB			
	Method	Denoiser	PESQ	CD	F-SNR	PESQ	CD	F-SNR	PESQ	CD	F-SNR	
WGN	Unprocessed	-	1.206	8.423	4.611	1.482	7.935	5.610	1.714	6.749	6.089	
	WPE	-	1.217	8.589	4.320	1.687	8.285	5.729	2.135	7.244	7.373	
	Conv-TasNet	-	0.667	9.109	4.377	1.635	8.255	5.699	1.805	7.288	5.696	
	Denoise + WPE	BLSTM		1.470	8.702	4.574	1.771	8.320	5.500	2.214	7.240	6.970
		DCUNet		0.937	8.467	4.565	1.499	8.045	5.522	1.614	6.780	6.251
		DCCNet		0.754	8.470	4.593	1.225	8.016	5.530	1.437	6.815	6.094
		FRCRN		1.773	8.507	4.469	1.419	8.151	5.447	2.169	7.126	5.788
	WPE + Denoise	BLSTM		1.461	8.001	3.677	1.606	7.471	4.978	1.978	6.506	5.976
		DCUNet		1.155	8.892	4.569	1.805	8.147	6.110	2.236	7.537	6.453
		DCCNet		0.714	9.677	3.928	1.546	9.413	5.476	2.209	8.394	6.051
		FRCRN		1.778	6.915	5.463	2.010	6.662	5.971	2.387	6.112	6.566
	PnPWPE	BLSTM		1.581	7.017	<b>5.992</b>	1.981	<b>6.382</b>	<u>7.023</u>	2.276	<u>5.360</u>	<u>7.843</u>
		DCUNet		1.222	8.382	4.945	1.854	7.739	6.509	2.372	6.432	7.755
		DCCNet		1.191	8.693	4.564	1.823	8.234	6.129	<b>2.397</b>	6.732	7.809
		FRCRN		<b>1.821</b>	<b>6.373</b>	<u>5.957</u>	<b>2.080</b>	<u>6.446</u>	<b>7.109</b>	2.325	<b>5.173</b>	7.582
Cafe	Unprocessed	-	1.334	6.879	3.493	1.572	6.295	4.457	1.671	5.760	5.460	
	WPE	-	1.383	7.057	3.263	1.887	6.169	4.498	2.087	4.991	6.007	
	Conv-TasNet	-	1.191	6.781	<b>4.963</b>	1.810	6.320	5.408	1.869	5.758	5.786	
	Denoise + WPE	BLSTM		0.962	6.845	3.437	1.573	6.424	4.039	1.858	5.532	6.392
		DCUNet		0.937	6.849	3.408	1.683	6.306	4.295	1.704	5.543	5.450
		DCCNet		0.754	6.871	3.393	1.579	6.288	4.230	1.650	5.700	5.266
		FRCRN		<u>1.472</u>	7.006	3.488	2.026	6.561	4.292	2.135	5.859	5.374
	WPE + Denoise	BLSTM		0.470	8.238	3.197	1.620	7.284	4.803	1.945	5.532	6.392
		DCUNet		1.170	7.795	4.280	1.735	7.175	5.383	2.062	6.759	6.415
		DCCNet		1.027	8.507	4.894	1.674	7.685	5.300	1.985	7.336	6.075
		FRCRN		1.138	<u>6.522</u>	4.830	1.976	5.993	<u>5.645</u>	<u>2.163</u>	5.225	<b>6.625</b>
	PnPWPE	BLSTM		1.370	6.817	3.818	<u>2.077</u>	7.284	4.803	2.112	4.881	6.372
		DCUNet		1.417	6.793	3.939	2.000	5.741	5.377	2.141	4.884	6.349
		DCCNet		<b>1.497</b>	6.637	4.500	2.033	<b>5.597</b>	<b>5.690</b>	2.125	4.848	6.412
		FRCRN		1.405	<b>6.478</b>	4.225	<b>2.083</b>	<u>5.657</u>	5.617	<b>2.261</b>	4.789	<u>6.515</u>
Babble	Unprocessed	-	1.284	6.715	3.117	1.515	6.360	4.274	1.653	5.757	5.185	
	WPE	-	1.622	6.871	2.801	1.802	6.068	4.141	2.100	4.846	5.847	
	Conv-TasNet	-	0.732	7.372	3.966	1.732	6.225	5.356	1.862	5.663	5.666	
	Denoise + WPE	BLSTM		0.940	6.767	2.988	1.381	8.372	3.885	1.674	5.618	4.879
		DCUNet		0.663	6.756	2.977	1.541	6.240	3.975	1.657	5.467	5.088
		DCCNet		0.957	6.752	2.967	1.653	6.246	3.980	1.709	5.674	4.897
		FRCRN		1.285	6.768	2.963	<b>1.977</b>	6.457	4.146	2.127	5.954	5.407
	WPE + Denoise	BLSTM		0.927	8.024	3.264	1.438	6.919	5.165	2.134	5.464	6.552
		DCUNet		0.840	8.321	3.213	1.631	7.203	5.234	2.002	6.424	6.780
		DCCNet		1.191	8.661	<u>3.547</u>	1.720	7.197	<u>5.836</u>	2.054	7.594	6.405
		FRCRN		1.001	7.048	3.514	1.866	<u>5.437</u>	<b>5.941</b>	2.121	4.399	6.800
	PnPWPE	BLSTM		1.443	<b>6.628</b>	<b>3.595</b>	1.936	5.653	5.209	2.161	4.660	6.584
		DCUNet		1.292	6.808	3.240	1.894	5.898	4.922	2.154	4.896	6.552
		DCCNet		1.541	6.805	3.311	1.913	5.872	5.012	<u>2.162</u>	4.937	6.312
		FRCRN		<b>1.796</b>	<u>6.683</u>	3.267	<u>1.947</u>	<b>5.355</b>	5.591	<b>2.239</b>	<b>4.334</b>	<b>6.998</b>

**WPE+denoise:** We compare PnPWPE with different intuitive concatenations of the vanilla WPE and DNN-based denoisers. The experimental results show the superiority of our proposed framework compared to the other concatenated strategies. To be more specific, from Table III and Table IV, it can be observed that PnPWPE surpasses Denoise+WPE and WPE+denoiser in most cases, as PnPWPE yields the most best and second best results of PESQ and CD in Room A and Room B. Especially in the scenarios with WGN, the superiority of PnPWPE becomes pronounced as it yields

all the best results. Even though in the several conditions with additive noise of people chattering, WPE+denoiser seems to perform better in terms of F-SNR, PnPWPE still maintains its merits if considering PESQ and CD. Taking the scenario of cafe noise (SNR = 0 dB) in Room A as an example, WPE+denoiser-DCCNet yields the best F-SNR among all the comparison methods. However, the PESQ and CD value of PnPWPE-DCCNet is **0.25** and **1.64** better than the former (**1.579**→**1.824**, **8.489**→**6.850**), respectively. The same phenomenon can be found among different denoisers

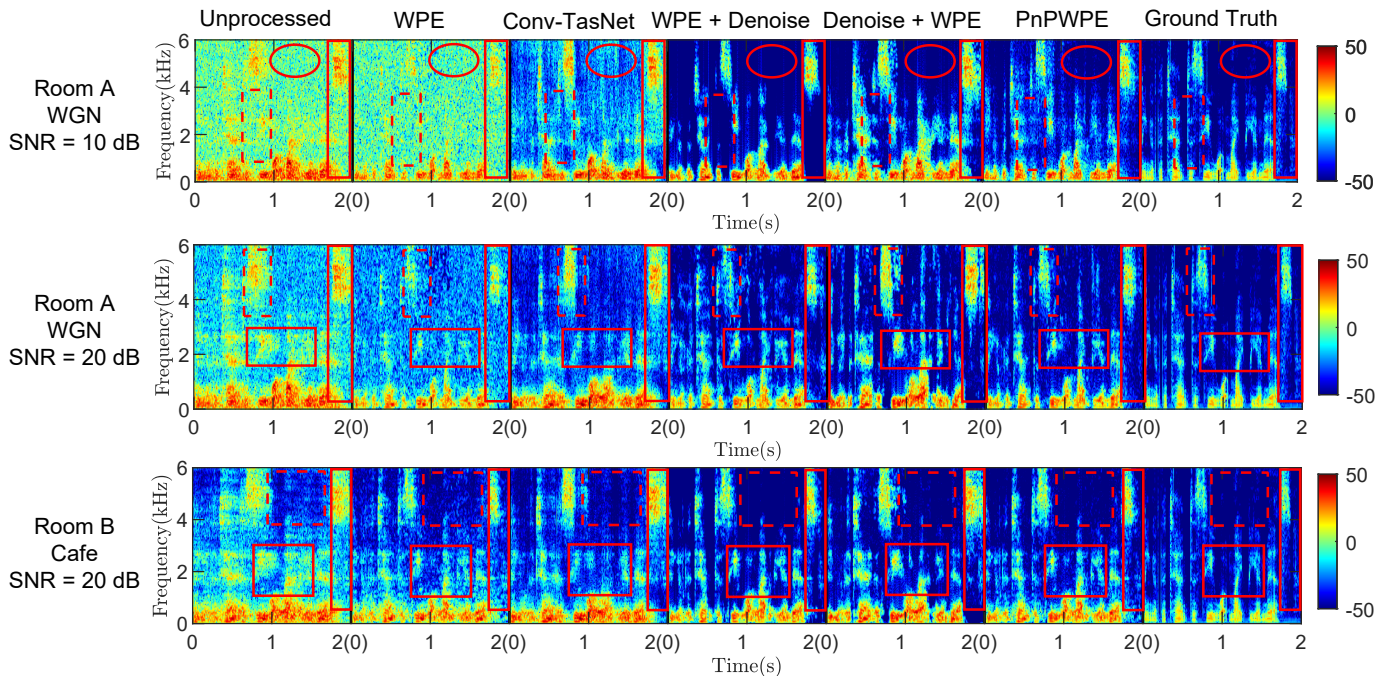


Fig. 4. The visualization results of all comparison methods with the speech truncated to 2 s. From left to right, we present the spectrograms of unprocessed speech, and the estimated speech processed by the vanilla WPE, Conv-TasNet, WPE + denoise, Denoise + WPE, PnPWPE and ground truth respectively.

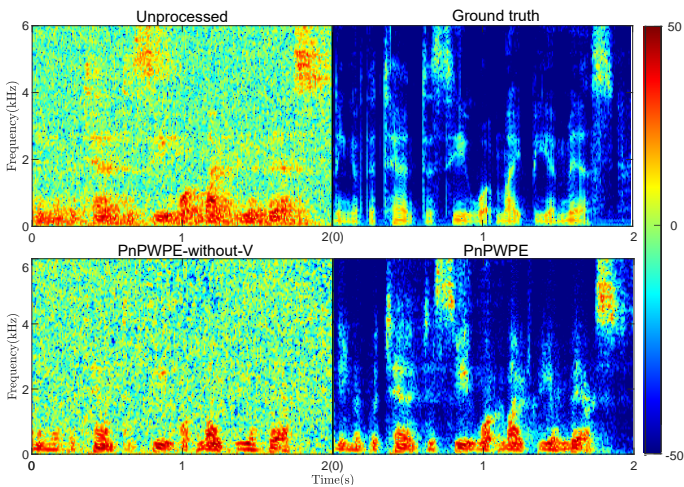


Fig. 5. The visualization results of PnPWPE and PnPWPE-without- $V$  under the scenario with WGN at SNR = 10 dB in Room A.

and different scenarios. In addition, we find `WPE+denoiser` usually performs better than `Denoise+WPE`, which is probably caused by the fact that denoising first could degrade the spatial property of the observed speech signals, and further impair the performance of the WPE method.

Examining Fig. 4, in the scenario involving white Gaussian noise (WGN) with low signal-to-noise ratio (SNR), the spectrogram of the estimated speech processed by `WPE+denoiser` reveals the presence of vertical lines (highlighted within an ellipse). These lines correspond to short and impulsive noises. Additionally, as indicated by the dotted rectangles in the figures, the subsequent denoising algorithm of `WPE+denoiser` tends to excessively cancel the additive noise, particularly in the high-frequency bands. This can result

in the loss of desired spectral components, ultimately impacting the quality of the estimated speech. On the other hand, when comparing `Denoise+WPE` to `PnPWPE`, we observe that the former fails to recover the desired speech from the observed input with the same level of detail. This difference can be observed by examining the solid line rectangles in Fig. 4. Based on these findings, we can conclude that our proposed framework, which incorporates deep speech priors, offers a more efficient approach to recovering speech from noisy and reverberant conditions compared to the intuitive concatenation of denoising and dereverberation algorithms.

**Discussion of  $V(n, k)$ :** In order to explore the capability of term  $V(n, k)$ , we conduct a comparison experiment between `PnPWPE` and `PnPWPE` without term  $V(n, k)$  (termed `PnPWPE-without- $V$` ), where the denoiser used here is `FR-CRN`. Fig. 5 and Fig. 6 present the bar plot and the evaluation results respectively. From Fig. 5, it is clear that `PnPWPE-without- $V$`  fails to remove the additive noise from the observed speech. Moreover, we can see from the bar plot in Fig. 6 that `PnPWPE-without- $V$`  is able to perform slightly better than the vanilla WPE in most cases, while the performance of `PnPWPE` improves significantly. For instance, the PESQ value of `PnPWPE` relatively exceeds that of `PnPWPE-without- $V$`  by around **20.6%**, **13.3%**, and **10.5%** in the scenarios of WGN, cafe and babble respectively. The same trend can be observed in term of CD and F-SNR. This is strong evidence that introducing the auxiliary term  $V(n, k)$  to our framework is reasonable. Further, from this comparison experiments, we can deduce that in addition to incorporating sophisticated speech prior for the framework, the capability of the DNN-based denoiser module in our proposed method is to eliminate some unknown and un-modelled noises, such as structural

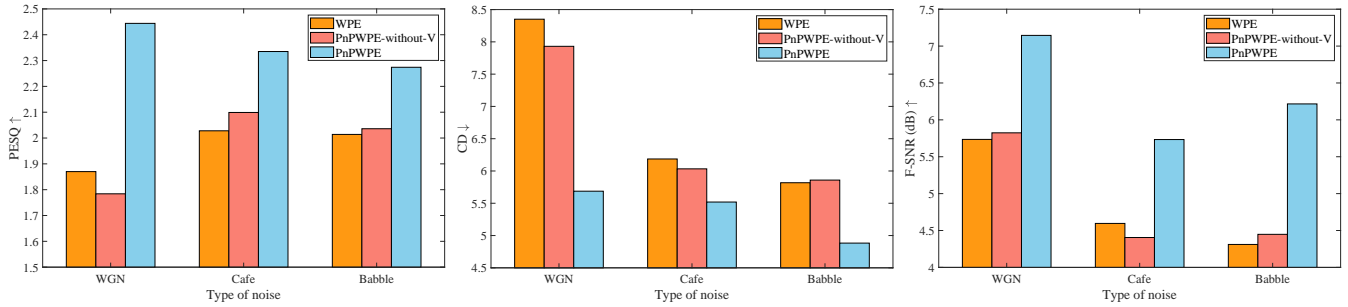


Fig. 6. The bar plot of all evaluation metrics in terms of PnPWPE and PnPWPE-without-V under the scenarios with all types of additive noises at SNR=10 dB in Room A. Here, we insert the FRCRN-based denoiser into the framework as an example.

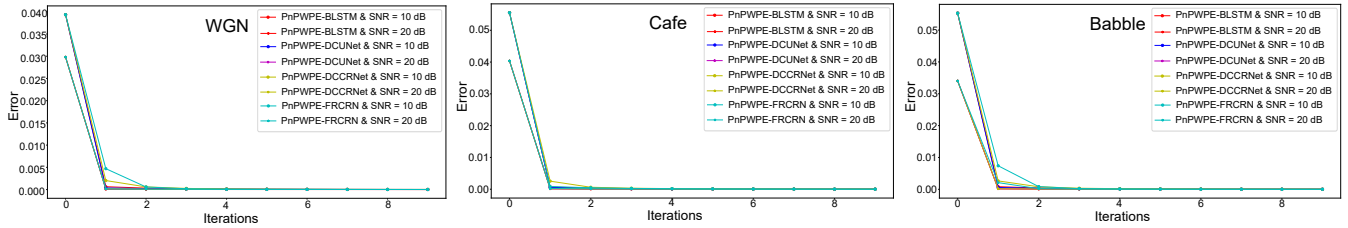


Fig. 7. The Error convergence curves of the proposed framework under the scenarios with all types of noises at SNR=10 dB and 20 dB in Room B.

noise during the optimization processing, instead of additive background noises [29].

**Convergence property of PnPWPE:** In our work, a DNN-based denoiser is utilized as a black-box to replace the explicitly solution of the subproblem in (32). The theoretical analysis of the convergence can be difficult, as nonlinear denoisers always involve complex operators, such as the BLSTM module. To illustrate the convergence, we present the convergence curves of our proposed framework of all DNN-based denoisers to experimentally show its convergence property. From Fig. 7, we observe that the proposed framework with each DNN-based denoiser has a stable and robust convergence property in terms of different types of noises. Besides, the proposed framework can reach stability after 3 iterations, demonstrating that an early stop operator can be performed to further save computation time consuming.

## V. CONCLUSION

In this paper, we have presented a method for improving the performance and robustness of the WPE algorithm in complex environments with reverberation and additive noise. Our approach integrates data-driven speech priors using a Plug-and-Play (PnP) strategy, specifically employing the RED strategy for speech reconstruction. We implemented various types of DNN-based denoisers and integrated them into the optimization steps, allowing us to effectively capture the prior information from data and demonstrate the flexibility of our proposed framework. The experimental results have confirmed the performance and robustness of our method under diverse conditions. However, there are several respects for future investigation:

- **Online and lightweight implementation:** It would be valuable to explore the development of an online and lightweight version of the proposed PnP method. As WPE is commonly employed in online scenarios for practical applications, adapting our framework to real-time settings would enhance its usability.

- **Alternative integration approaches:** Further research can be conducted to investigate alternative ways of integrating data-driven approaches. For instance, instead of using denoisers, inserting a generative module, or employing other strategies for integrating data-driven approaches can be explored like in [30].
- **Extension to other speech processing tasks:** The combination of physics-based and data-driven approaches holds promise for addressing various speech processing tasks beyond dereverberation. By employing the proposed PnP strategy, other tasks can leverage denoisers to capture speech priors, eliminating the need for training task-dependent networks.

## REFERENCES

- [1] S. R. Chetupalli and T. V. Sreenivas, "Late reverberation cancellation using bayesian estimation of multi-channel linear predictors and student's t-source prior," *IEEE/ACM Trans. Audio, Speech, Lang. Process.*, vol. 27, no. 6, pp. 1007–1018, Mar. 2019.
- [2] V. Kothapally and J. HL Hansen, "Skipconvgan: Monaural speech dereverberation using generative adversarial networks via complex time-frequency masking," *IEEE/ACM Trans. Audio, Speech, Lang. Process.*, vol. 30, pp. 1600–1613, Mar. 2022.
- [3] H. Kuttruff, *Room acoustics*, Crc Press, 2016.
- [4] P. A. Naylor *et al.*, *Speech dereverberation*, vol. 2, Springer, 2010.
- [5] D. Schmid, G. Enzner, S. Malik, D. Kolossa, and R. Martin, "Variational bayesian inference for multichannel dereverberation and noise reduction," *IEEE/ACM Trans. Audio, Speech, Lang. Process.*, vol. 22, no. 8, pp. 1320–1335, Aug. 2014.
- [6] K. Kinoshita *et al.*, "The reverb challenge: A common evaluation framework for dereverberation and recognition of reverberant speech," in *Proc. IEEE Workshop Appl. Signal Process. to Audio Acoust.* IEEE, 2013, pp. 1–4.
- [7] I. Kodrasi and S. Doclo, "Joint dereverberation and noise reduction based on acoustic multi-channel equalization," *IEEE/ACM Trans. Audio, Speech, Lang. Process.*, vol. 24, no. 4, pp. 680–693, Apr. 2016.
- [8] I. Kodrasi and S. Doclo, "Analysis of eigenvalue decomposition-based late reverberation power spectral density estimation," *IEEE/ACM Trans. Audio, Speech, Lang. Process.*, vol. 26, no. 6, pp. 1106–1118, Jun. 2018.
- [9] G. Huang, J. Benesty, I. Cohen, and J. Chen, "A simple theory and new method of differential beamforming with uniform linear microphone arrays," *IEEE/ACM Trans. Audio, Speech, Lang. Process.*, vol. 28, pp. 1079–1093, Mar. 2020.

- [10] T. Nakatani, B.-H. Juang, T. Yoshioka, K. Kinoshita, M. Delcroix, and M. Miyoshi, "Speech dereverberation based on maximum-likelihood estimation with time-varying Gaussian source model," *IEEE/ACM Trans. Audio, Speech, Lang. Process.*, vol. 16, no. 8, pp. 1512–1527, Nov. 2008.
- [11] T. Nakatani, T. Yoshioka, K. Kinoshita, M. Miyoshi, and B.-H. Juang, "Speech dereverberation based on variance-normalized delayed linear prediction," *IEEE/ACM Trans. Audio, Speech, Lang. Process.*, vol. 18, no. 7, pp. 1717–1731, Sep. 2010.
- [12] A. Jukić and S. Doclo, "Speech dereverberation using weighted prediction error with laplacian model of the desired signal," in *Proc. IEEE Int. Conf. Acoust., Speech, Signal Process.* IEEE, 2014, pp. 5172–5176.
- [13] B. Schwartz, S. Gannot, and E. A. Habets, "Online speech dereverberation using kalman filter and em algorithm," *IEEE/ACM Trans. Audio, Speech, Lang. Process.*, vol. 23, no. 2, pp. 394–406, Nov. 2014.
- [14] Z. Wang and D. Wang, "Deep learning based target cancellation for speech dereverberation," *IEEE/ACM Trans. Audio, Speech, Lang. Process.*, vol. 28, pp. 941–950, Feb. 2020.
- [15] S. Braun *et al.*, "Evaluation and comparison of late reverberation power spectral density estimators," *IEEE/ACM Trans. Audio, Speech, Lang. Process.*, vol. 26, no. 6, pp. 1056–1071, Jun. 2018.
- [16] A. Jukić, T. van W., T. Gerkmann, and S. Doclo, "Multi-channel linear prediction-based speech dereverberation with sparse priors," *IEEE/ACM Trans. Audio, Speech, Lang. Process.*, vol. 23, no. 9, pp. 1509–1520, Jun. 2015.
- [17] M. Witkowski and K. Kowalczyk, "Split bregman approach to linear prediction based dereverberation with enforced speech sparsity," *IEEE Signal Process. Lett.*, vol. 28, pp. 942–946, Apr. 2021.
- [18] D. Wang and J. Chen, "Supervised speech separation based on deep learning: An overview," *IEEE/ACM Trans. Audio, Speech, Lang. Process.*, vol. 26, no. 10, pp. 1702–1726, May. 2018.
- [19] K. Han *et al.*, "Learning spectral mapping for speech dereverberation and denoising," *IEEE/ACM Trans. Audio, Speech, Lang. Process.*, vol. 23, no. 6, pp. 982–992, Mar. 2015.
- [20] M. Mimura, S. Sakai, and T. Kawahara, "Speech dereverberation using long short-term memory," in *Proceedings of interspeech*, 2015.
- [21] Y. Luo, Z. Chen, and T. Yoshioka, "Dual-path RNN: efficient long sequence modeling for time-domain single-channel speech separation," in *Proc. IEEE Int. Conf. Acoust., Speech, Signal Process.* IEEE, 2020, pp. 46–50.
- [22] B. J. Borgström and M. S. Brandstein, "Speech enhancement via attention masking network (seamnet): An end-to-end system for joint suppression of noise and reverberation," *IEEE/ACM Trans. Audio, Speech, Lang. Process.*, vol. 29, pp. 515–526, Dec. 2020.
- [23] Y. Zhao, D. Wang, B. Xu, and T. Zhang, "Monaural speech dereverberation using temporal convolutional networks with self attention," *IEEE/ACM Trans. Audio, Speech, Lang. Process.*, vol. 28, pp. 1598–1607, May 2020.
- [24] Z. Wang, G. Wichern, and J. Le Roux, "Convolutional prediction for monaural speech dereverberation and noisy-reverberant speaker separation," *IEEE/ACM Trans. Audio, Speech, Lang. Process.*, vol. 29, pp. 3476–3490, Nov. 2021.
- [25] N. Shlezinger, Y. C. Eldar, and S. P. Boyd, "Model-based deep learning: On the intersection of deep learning and optimization," *arXiv preprint arXiv:2205.02640*, 2022.
- [26] Y. Bai, W. Chen, J. Chen, and S. Guo, "Deep learning methods for solving linear inverse problems: Research directions and paradigms," *Signal Processing*, vol. 177, pp. 107729 (23 pages), 2020.
- [27] V. Monga, Y. Li, and Y. C. Eldar, "Algorithm unrolling: Interpretable, efficient deep learning for signal and image processing," *IEEE Signal Process. Mag.*, pp. 18–44, 2021.
- [28] S. H. Chan, X. Wang, and O. A. Elgendy, "Plug-and-play ADMM for image restoration: Fixed-point convergence and applications," *IEEE Trans. Comput. Imaging*, vol. 3, no. 1, pp. 84–98, 2016.
- [29] K. Zhang, Y. Li, W. Zuo, L. Zhang, L. Van Gool, and R. Timofte, "Plug-and-play image restoration with deep denoiser prior," *IEEE Trans. Pattern Anal. and Mach. Intell.*, June. 2021.
- [30] J. Chen, M. Zhao, X. Wang, C. Richard, and S. Rahardja, "Integration of physics-based and data-driven models for hyperspectral image unmixing: A summary of current methods," *IEEE Signal Process. Mag.*, vol. 40, no. 2, pp. 61–74, Feb. 2023.
- [31] X. Wang, J. Chen, Q. Wei, and C. Richard, "Hyperspectral image super-resolution via deep prior regularization with parameter estimation," *IEEE Trans. Circuits Syst. Video Technol.*, vol. 32, no. 4, pp. 1708–1723, 2021.
- [32] M. Zhao, X. Wang, J. Chen, and W. Chen, "A plug-and-play priors framework for hyperspectral unmixing," *IEEE Trans. Geosc. Remote Sens.*, vol. 60, pp. 1–13, Jan. 2021.
- [33] R. Ahmad, C. A. Bouman, G. T. Buzzard, S. Chan, S. Liu, E. T. Reehorst, and P. Schniter, "Plug-and-play methods for magnetic resonance imaging: Using denoisers for image recovery," *IEEE signal process. mag.*, vol. 37, no. 1, pp. 105–116, 2020.
- [34] K. Kinoshita, M. Delcroix, H. Kwon, T. Mori, and T. Nakatani, "Neural network-based spectrum estimation for online wpe dereverberation," in *Proceedings of interspeech*, 2017, pp. 384–388.
- [35] J. Heymann, L. Drude, R. Haeb-Umbach, K. Kinoshita, and T. Nakatani, "Joint optimization of neural network-based wpe dereverberation and acoustic model for robust online asr," in *Proc. IEEE Int. Conf. Acoust., Speech, Signal Process.* IEEE, 2019, pp. 6655–6659.
- [36] Y. Romano, M. Elad, and P. Milanfar, "The little engine that could: Regularization by denoising (RED)," *SIAM J. Imaging Sci.*, vol. 10, no. 4, pp. 1804–1844, 2017.
- [37] X. Wang, J. Chen, C. Richard, and D. Brie, "Learning spectral-spatial prior via 3DDNCNN for hyperspectral image deconvolution," in *Proc. IEEE Int. Conf. Acoust., Speech, Signal Process.* IEEE, 2020, pp. 2403–2407.
- [38] H.-S. Choi, J.-H. Kim, J. Huh, A. Kim, J.-W. Ha, and K. Lee, "Phase-aware speech enhancement with deep complex u-net," in *Int. Conf. on Learn. Representations*, Sep. 2019.
- [39] J. Cosentino, M. Pariente, S. Cornell, A. Deleforge, and E. Vincent, "Librimix: An open-source dataset for generalizable speech separation," *arXiv preprint arXiv:2005.11262*, 2020.
- [40] Y. Hu, Y. Liu, S. Lv, M. Xing, S. Zhang, Y. Fu, J. Wu, B. Zhang, and L. Xie, "DCCRN: Deep complex convolution recurrent network for phase-aware speech enhancement," *arXiv preprint arXiv:2008.00264*, Sep. 2020.
- [41] S. Zhao, B. Ma, K. N. Watcharasupat, and W.-S. Gan, "Frcrn: Boosting feature representation using frequency recurrence for monaural speech enhancement," in *Proc. IEEE Int. Conf. Acoust., Speech, Signal Process.* IEEE, May 2022, pp. 9281–9285.
- [42] H. Dubey *et al.*, "ICASSP 2022 deep noise suppression challenge," in *Proc. IEEE Int. Conf. Acoust., Speech, Signal Process.* IEEE, May 2022, pp. 9271–9275.
- [43] C. Xu, W. Rao, E. S. Chng, and H. Li, "Optimization of speaker extraction neural network with magnitude and temporal spectrum approximation loss," in *Proc. IEEE Int. Conf. Acoust., Speech, Signal Process.*, 2019, pp. 6990–6994.
- [44] A. Varga and H. J. Steeneken, "Assessment for automatic speech recognition: Ii. noisex-92: A database and an experiment to study the effect of additive noise on speech recognition systems," *Speech communication*, vol. 12, no. 3, pp. 247–251, July 1993.
- [45] J. Barker, R. Marxer, E. Vincent, and S. Watanabe, "The third 'chime' speech separation and recognition challenge: Dataset, task and baselines," in *2015 IEEE Workshop on Automatic Speech Recognition and Understanding (ASRU)*. IEEE, Dec 2015, pp. 504–511.
- [46] J. Garofolo, D. Graff, D. Paul, and D. Pallett, "Csr-i (wsj0) complete ldc93s6a," *Web Download. Philadelphia: Linguistic Data Consortium*, vol. 83, 1993.
- [47] D. P. Kingma and J. Ba, "Adam: A method for stochastic optimization," *arXiv preprint arXiv:1412.6980*, 2014.
- [48] P. Ronneberger, O. Fischer, and T. Brox, "U-net: Convolutional networks for biomedical image segmentation," in *Medical Image Computing and Computer-Assisted Intervention (MICCAI)*. Springer, Oct. 2015, pp. 234–241.
- [49] Y. Luo and N. Mesgarani, "Conv-tasnet: Surpassing ideal time-frequency magnitude masking for speech separation," *IEEE/ACM Trans. Audio, Speech, Lang. Process.*, vol. 27, no. 8, pp. 1256–1266, May 2019.
- [50] M. Maciejewski, G. Wichern, E. McQuinn, and J. Le Roux, "Wham!: Noisy and reverberant single-channel speech separation," in *Proc. IEEE Int. Conf. Acoust., Speech, Signal Process.* IEEE, May 2020, pp. 696–700.
- [51] A. W. Rix, J. G. Beerends, M. P. Hollier, and A. P. Hekstra, "Perceptual evaluation of speech quality (PESQ)-a new method for speech quality assessment of telephone networks and codecs," in *Proc. IEEE Int. Conf. Acoust., Speech, Signal Process.*, 2001, vol. 2, pp. 749–752.
- [52] K. Kinoshita *et al.*, "A summary of the reverberant challenge: state-of-the-art and remaining challenges in reverberant speech processing research," *EURASIP J. Adv. Signal Process.*, vol. 2016, no. 1, pp. 1–19, 2016.
- [53] J. B. Allen and D. A. Berkley, "Image method for efficiently simulating small-room acoustics," *J. Acoust. Soc. Am.*, vol. 65, no. 4, pp. 943–950, June 1979.
- [54] V. Panayotov, G. Chen, D. Povey, and S. Khudanpur, "Librispeech: an asr corpus based on public domain audio books," in *Proc. IEEE Int. Conf. Acoust., Speech, Signal Process.* IEEE, Apr. 2015, pp. 5206–5210.

- [55] G. Huang, J. Benesty, I. Cohen, and J. Chen, “Kronecker product multichannel linear filtering for adaptive weighted prediction error-based speech dereverberation,” *IEEE/ACM Trans. Audio, Speech, Lang. Process.*, vol. 30, pp. 1277–1289, Mar. 2022.